

ERS Satellite Microwave Radar Observations of Antarctic Sea-Ice Dynamics

Mark R. Drinkwater Jet Propulsion Laboratory, California Institute of Technology,
4800 Oak Grove Drive, Pasadena, CA 91109, USA

mrd@pacific.jpl.nasa.gov
http://ftp-oceans.jpl.nasa.gov/mrd/Marks_Homepage.html

Xiang Liu Jet Propulsion Laboratory, California Institute of Technology,
4800 Oak Grove Drive, Pasadena, CA 91109, USA

xiang@pacific.jpl.nasa.gov
http://ftp-oceans.jpl.nasa.gov/mrd/JPL_polar_gen.html

Abstract

ERS-1 and ERS-2 scatterometer and SAR data are used to monitor and track large and small-scale sea-ice dynamics in the Southern Ocean, and in particular in the Weddell Sea, Antarctica. Sea-ice formation in the Weddell Sea regulates vertical and horizontal thermohaline circulation and influences bottom water production rates. Significant seasonal to interannual variability is observed in the sea-ice drift dynamics. Coupled model simulations reproduce this variability and indicate that there is significant interannual variability in Weddell Sea ice formation, drift and extent on the ENSO timescale, with a period of ~ 8 years. Changes in ice dynamics on these timescales regulate the amount of sea-ice divergence and polynya formation. Anomalies in timing and duration of the opening of the Ronne ice-shelf polynya system are closely related to the variability in outflow of Weddell Sea bottom water measured at Joinville Island.

Keywords: Antarctic, SAR images, sea-ice dynamics, Ronne Polynya, Weddell Polynya, Antarctic Circumpolar Wave

Introduction

Ocean-atmosphere exchanges are exaggerated when the Antarctic sea-ice cover is parted and the ocean exposed to brisk winds. Relative sea-ice motions and lead formation occur under tidal shear or conditions of high wind-stress divergence, and large resulting fluxes of sensible and latent heat cause rapid ice growth in leads and polynyas. Resulting production of cold, salty shelf water participates in Antarctic bottom-water formation, and to some extent in driving horizontal and vertical thermohaline circulation. The majority of mixing and heat exchange in the ocean boundary layer is induced by momentum transfer to the sea ice surface during frequent storm bursts, and especially during the passage of fast-moving low pressure systems. Noteworthy periods of dynamic-thermodynamic changes in the ice cover, however, are more often

than not accompanied by a blanket of cloud due to atmospheric radiation-feedback mechanisms. In these cases, the atmosphere is inherently more electromagnetically opaque, and retrievals of ice characteristics information using satellite passive microwave algorithms are called into question. Recent studies indicate that traditional ice concentration estimates can be in error by values exceeding 10% under typical storm conditions.

In this paper, we document some of the characteristics and variability in sea ice in the Weddell Sea, Antarctica. We show how dynamics regulate the opening and closing, and in redistribution of the pack ice in response to forcing. Comparisons with model simulated data and meteorological fields indicate that the basin-scale circulation is closely coupled with atmospheric forcing. Interannual variability in ice dynamics and ice production rates are observed in response to 4-year climate anomalies originating in the South Pacific from the 'El Niño' southern oscillation. These impulses are transmitted around Antarctica via sea-surface temperature anomalies in the Antarctic Circumpolar Current, and changes in the general atmospheric circulation.

Dataset

Since 1991, ERS-1 and ERS-2 are the only other uninterrupted source of weather-independent radar images of the Southern Ocean sea-ice cover in Antarctica. Both the Synthetic Aperture Radar (SAR) and Scatterometer modes of the C-band Active Microwave Instrument on board ERS, have been used to generate a radar image database spanning the period 1992-present day. Together, these combined microwave data enable almost uninterrupted imaging of the geographic region shown in Figure 1, with global coverage with medium-scale (~20 km) enhanced resolution scatterometer images (Drinkwater *et al.*, 1993), and limited mesoscale coverage at high resolution (25m) SAR images. Together, these combined radar datasets are now routinely used to measure ice kinematics and surface conditions in response to meteorological forcing, using JPL-developed automated algorithms developed for use at the Alaska SAR Facility.

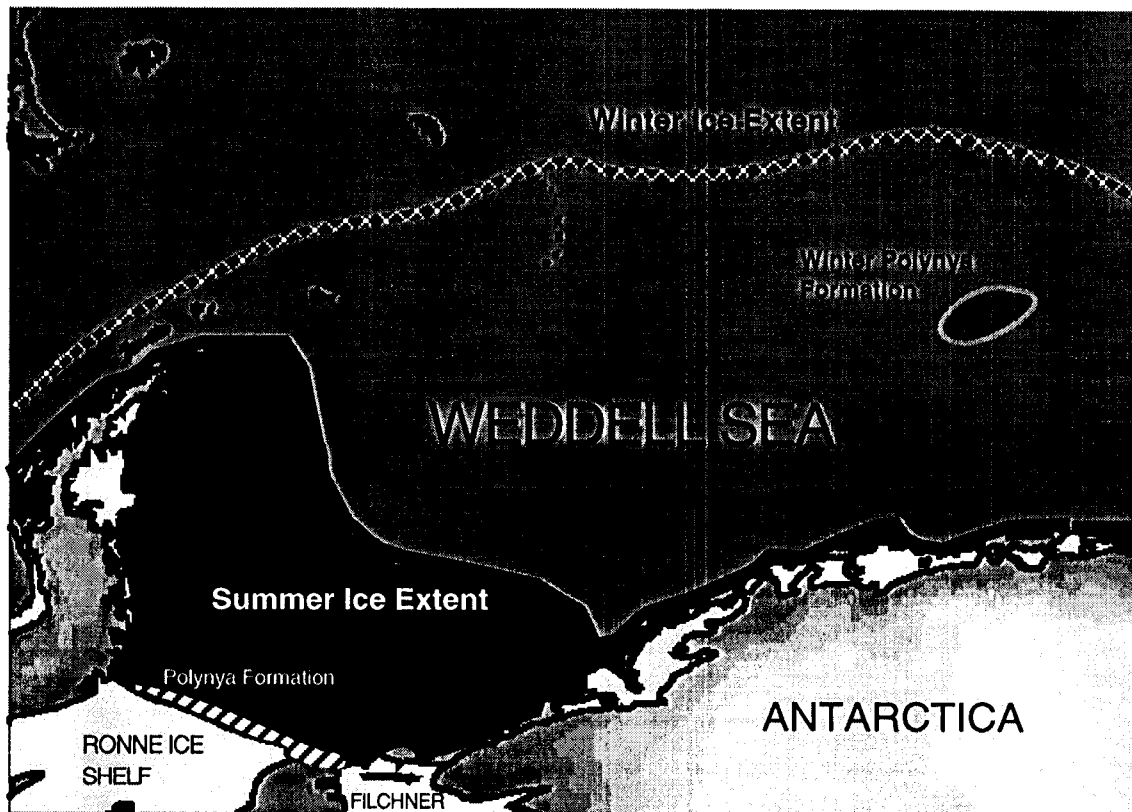


Figure 1. Schematic diagram showing main characteristics of the seasonal ice extent, and two primary locations of polynya formation, in the Weddell Sea, Antarctica.

Ice Motion Response to Wind Forcing

During 1992, several buoys were deployed in the eastern Weddell Sea as part of the WWGS '92 experiment, in a region comprised of level, undeformed white ice. Simultaneous overlapping SAR acquisitions were planned in July 1992 such that the buoys could be used as validation for the SAR motion retrievals. Under divergent conditions in the Central Weddell Sea, and consequently relatively free drift, the majority of ice drift vectors observed by SAR in the vicinity of the buoy array follow a pattern expected from Ekman dynamics. Figure 2 shows 3-day SAR-observed drift vectors together with the corresponding WWGS '92 buoy drift tracks marked as dotted Lagrangian trajectories. The superimposed pressure field is optimally interpolated using a polynomial scheme which combines weighted buoy pressure measurements together with 1000 mB ECMWF pressure analysis fields. This technique was originally used by Kottmeier and Sellmann (1996) but is hybridized here by extending and constraining the fitting procedure to broaden the geographic limits, to include synoptic-scale features and the SAR-tracked domain. Corresponding gridded geostrophic winds are indicated together with optimally interpolated climatological mean geostrophic currents derived from original data supplied by Kottmeier and Sellmann (1996).

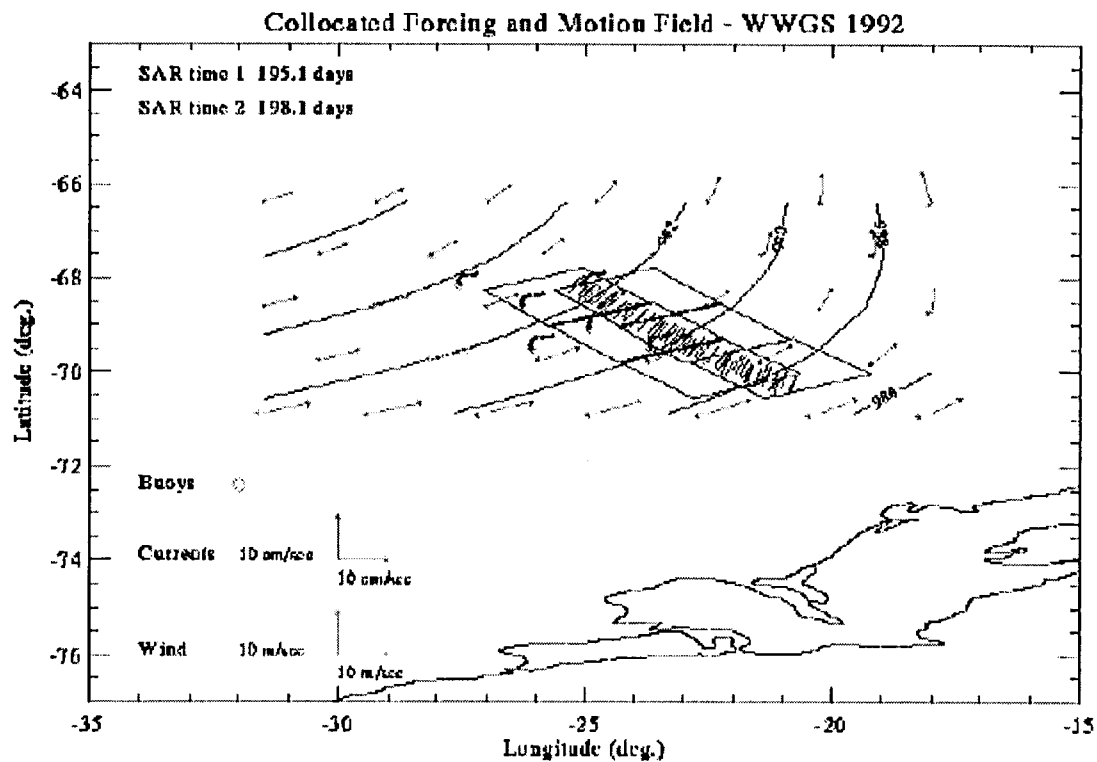


Figure 2. SAR-derived ice motion superimposed on the WWGS '92 buoy drift array, for period 13-16 July, 1992. Gridded geostrophic winds and mean climatological geostrophic currents are shown together with the optimally interpolated ECMWF pressure field. Buoy start locations are identified by '♦' symbols.

Episodic bouts of divergence and convergence are observed primarily in response to storm impulses at the leading and trailing edges of low pressure systems, respectively. Figure 2 shows the mean synoptic and ice-motion situation accompanying the ice drift in this region of the central Weddell Sea. The passing trough of low pressure causes a rapid adjustment in the buoy drift, each buoy exhibiting a 90° direction change in direction over the 3-day period of ice tracking. Geostrophic winds are observed to change from southerlies to westerlies during this interval, as a consequence of the eastward passage of the low pressure trough, while the SAR motion vectors show a convergence in response to winds which become southerly with proximity to the Antarctic coast. Lagged cross correlations between wind and ice drift indicate that the ice drift has a response time of around 12 hours to the passage of storms such as that illustrated in Figure 2 (Drinkwater, 1996).

Results

New ice kinematics datasets yield a variety of important new information on the seasonal to interannual variability in Antarctic ice dynamics, and the processes linking storms with mesoscale ice divergence. 3-day gridded SAR and Scatterometer ice-motion fields are validated using buoy drift trajectories, and combinations of entire years of ice motion were used to derive climatological mean ice motion. Figure 3 shows the mean 12-monthly climatological sea-ice drift for 1992, constructed from over 100 individual 3-

day ice motion products, each derived by automated tracking of sea ice in pairs of ERS-1 scatterometer images.

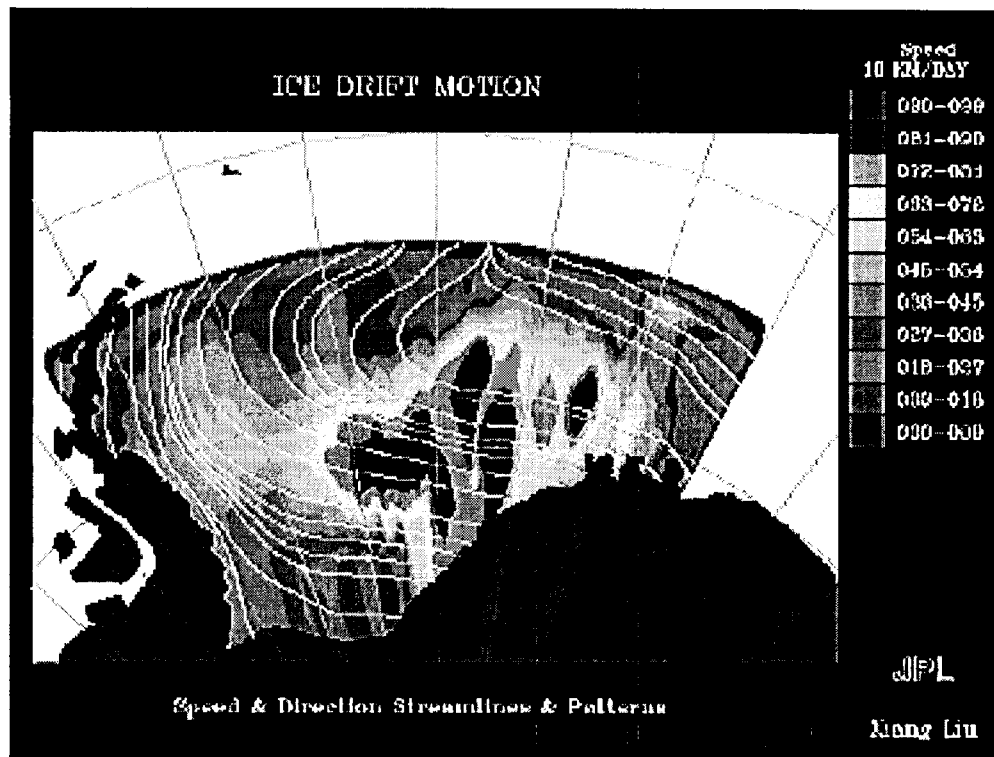


Figure 3. Weddell Sea climatological mean ice drift for 1992, derived from ERS-1 scatterometer 3-day ice drift data. White lines indicate streamlines of drift, and the color coding indicates the drift speed.

Periods of high wind-stress divergence result in regional openings of the ice cover and notably a brief reappearance of the winter Weddell Polynya in 1994, which was first discovered in ERS-1 scatterometer images (Figure 4), and confirmed using SAR data acquired during a shipborne experiment in the Maud Rise region. These data are presently being analysed in conjunction with SSM/I passive microwave radiometer data and oceanographic data acquired during the Anzflux experiment [McPhee *et al.*, 1996].

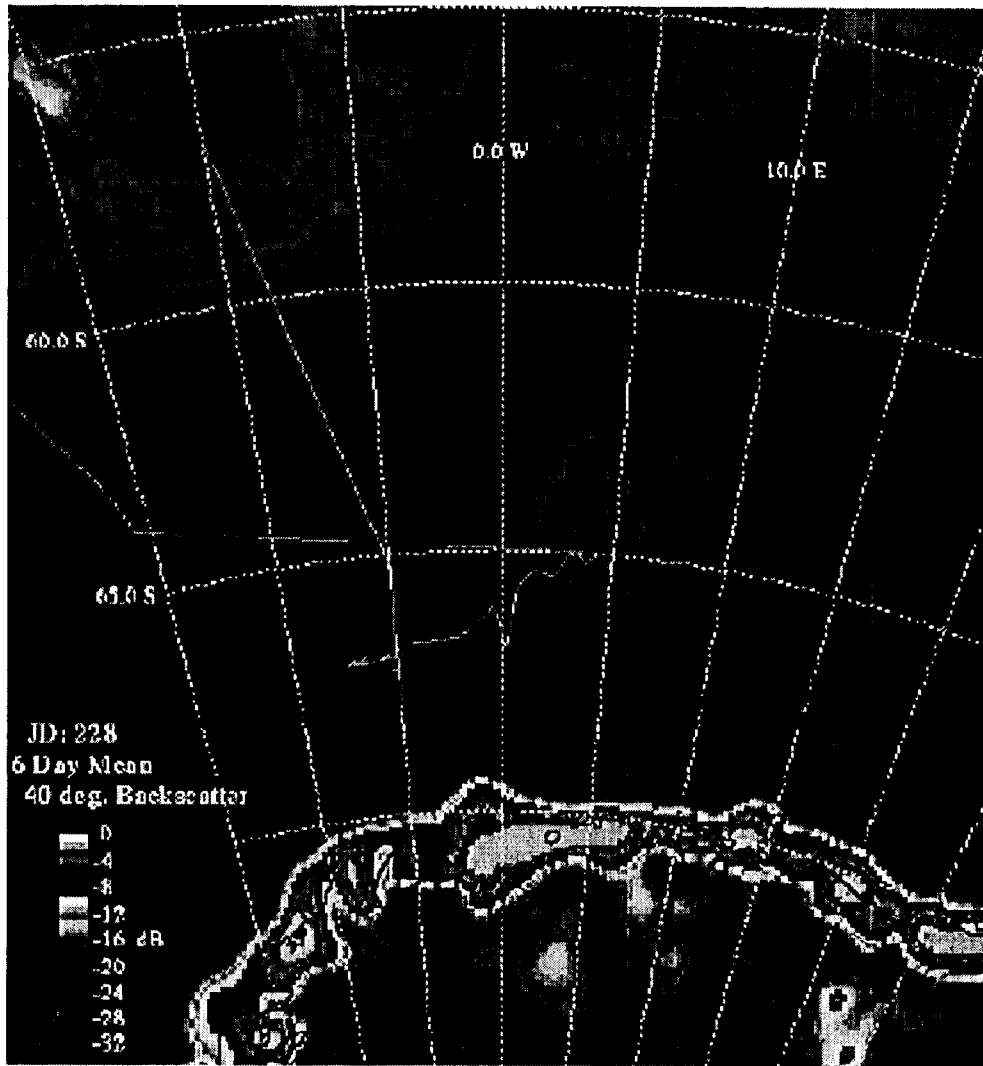


Figure 4. Reappearance of the Weddell Polynya in scatterometer image August 1994. The orange line indicates the cruise track of the Nathaniel Palmer during the Anzflux experiment.

Comparison between tracked ice-motion fields and simulation results from a dynamic-thermodynamic model indicate a large degree of variability in both seasonal and annual mean ice drift. This variability in turn appears to be strongly coupled to anomalies in sea-level pressure and meridional wind stress observed in ECMWF meteorological analysis fields (White and Petersen, 1996). Dynamic-thermodynamic model simulations reproduce seasonal variability in ice drift and indicate that there is significant interannual variability in Weddell Sea ice formation, and drift and on the El Niño Southern Oscillation (ENSO) timescale, with a period of ~ 8 years. This variability is consistent with the eastward passing of a spatial pattern of linked atmospheric and sea-surface temperature anomalies, characterised by White and Petersen (1996) as an “Antarctic Circumpolar Wave”.

Changes in ice dynamics on these timescales regulate the amount of sea-ice divergence and ice-shelf polynya formation, in particular along the Ronne ice shelf. Appearance of a large polynya in this region was previously documented by Drinkwater *et al.* (1993) in both SAR and scatterometer data. The timing and

duration of the opening of the Ronne ice-shelf polynya system is strongly regulated by the meridional wind stress, since this carries ice northwards away from the ice-shelf front. Divergence and open-water formation in this location enables ice production in excess of 7 m per year, in contrast to the typical thickness of ~1m ice found elsewhere in the Weddell Sea. The measured outflow of cold Antarctic bottom water appears to be closely related to the ice production and salt rejection during polynya formation events. Figure 5 shows the relationship between the seasonal and annual mean Weddell Sea Bottom Water outflow [Fahrbach *et al.*, 1995], and the filtered Net Freezing Rate anomaly, calculated with a dynamic-thermodynamic sea-ice model [Kreyscher, *pers. comm.*].

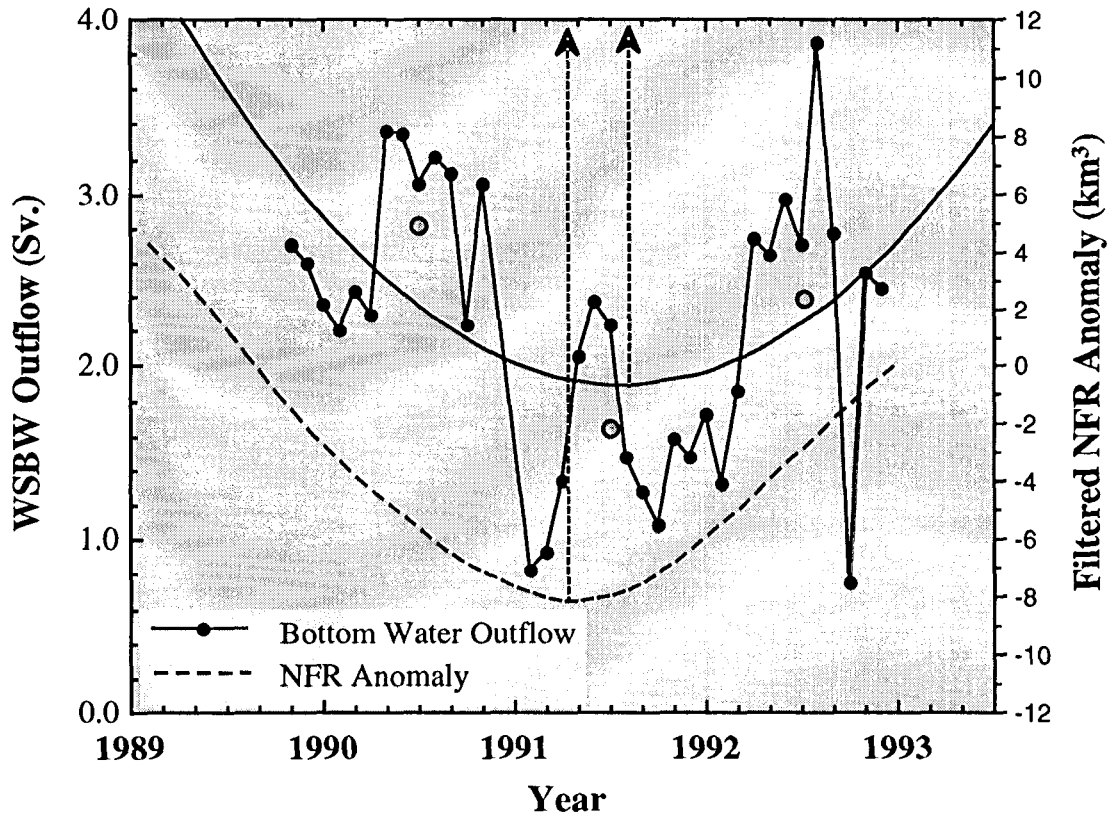


Figure 5. Comparison between filtered Net Freezing Rate (NFR) anomaly and Weddell Sea bottom water outflow at Joinville Island (after Fahrbach *et al.*, 1995). Arrows indicate lag between these interannual cycles.

The upper fitted 2nd order polynomial curve in Figure 5 indicates the general long-term variations in Weddell Sea bottom water outflow, superimposed on the seasonal mean outflow (jagged black line) and mean annual outflow record (represented by large circle symbols). The lower blue net freezing rate anomaly (NFR) cycle is calculated over the period 1986-1993 by removing the annual mean cycle from the monthly integrated ice production record within a number of model grid cells in the Southern Weddell Sea (spanning the region of Ronne polynya formation). This curve is filtered using a 3-year admittance window and indicates a 4-year peak-to-peak anomaly cycle in response to changes in the forcing over these timescales. In summary, Figure 5 indicates that the bottom water flowing out of the Weddell Sea into the global abyssal ocean, is controlled by climate-regulated sea-ice dynamics in the Weddell Sea. Since the Weddell Sea is the

primary bottom water formation region, it is anticipated that interannual anomalies in outflow have a considerable impact on global thermohaline circulation.

Conclusions

ERS-1 and 2 microwave radar observations in the Southern Ocean are actively contributing towards revolutionizing the study of Antarctic sea-ice geophysics. Seasonal patterns of global sea-ice drift together with the accompanying transitions in sea-ice characteristics can now be accurately characterized. More SAR data must be acquired in other seasons and locations to enhance the high-resolution coverage of the Weddell Sea at times when the O'Higgins receiving station has not previously been opened. Nonetheless, scatterometer images have been widely utilised to fill in the space and time gaps existing in the SAR image record.

The longer high-resolution satellite radar records become extended, the better the chances of measuring climate-anomaly-related Antarctic sea-ice variability on timescales equal to or exceeding the duration of a satellite mission. Only then can statistical relationships between forcing and dynamic-thermodynamic response be established for interannual to decadal timescale variability. Our preliminary results only hint at teleconnections between the mid- and high latitude oceans via the sea-ice cover around Antarctica. As the era of microwave remote sensing continues, extended datasets must be widely employed in confirming or denying these preliminary findings via long-term, large-scale observation records of the Antarctic sea ice cover.

Acknowledgments

This work was conducted by MRD and XL at Jet Propulsion Laboratory, California Institute of Technology, under contract to NASA. Funding support was provided by Robert Thomas (Code YSG) in the NASA Office for Mission to Planet Earth. Martin Kreyscher kindly produced the model simulations of Weddell Sea ice production and dynamics, while visiting JPL under support from a German DAAD scholarship.

References

- Drinkwater, M.R., In Press, Satellite Microwave Radar Observations of Antarctic Sea Ice. In C. Tsatsoulis and R. Kwok (Eds.), *Recent Advances in the Analysis of SAR for Remote Sensing of the Polar Oceans*, Springer Verlag, submitted 1996.
- Drinkwater, M. R., Long, D. G., and Early, D. S., 1993. Enhanced Resolution Scatterometer Imaging of Southern Ocean Sea Ice, *ESA Journal*, **17**, 307-322.
- Fahrbach, E., G. Rohardt, N. Scheele, M. Schröder, V. Strass, and A. Wisotzki, 1995. Formation and Discharge of Deep and Bottom Water in the Northwestern Weddell Sea, *J. Mar. Res.*, **53**, 515-538.
- Kottmeier, C., and L. Sellmann, 1996. Atmospheric and Oceanic Forcing of Weddell Sea Ice Motion, *J. Geophys. Res.*, **101**, C9, 20809-20824.
- McPhee, M.G., S.F. Ackley, P. Guest, B.A. Huber, D.G. Martinson, J.H. Morison, R.D. Muench, L. Padman, and T.P. Stanton, 1996. The Antarctic Zone Flux Experiment, *Bull Am. Met. Soc.*, **77**, 6, 1221-1232.